Progress In Electromagnetics Research, PIER 9, 181–218, 1994

ELECTROMAGNETIC WAVES IN PLANAR INTEGRATED PSEUDOCHIRAL Ω STRUCTURES

A. Toscano and L. Vegni

1. Introduction

Planar layered structures have played a significant role in microwave technology [see for example 1, 2]. This role is increasing day by day thanks to the investigations of new configurations (including different geometries or anisotropic substrates) as well as to the advances in material technology [3–5].

Printed antenna problems involving stratified complex substrates have also been a matter of particular attention in recent years. It has been demonstrated that, by properly choosing the layer thickness and

material parameters, significant improvements can be achieved in the performance of the printed antennas including the reduction or elimination of surface waves. Also, a double layer structure allows for the separation of active circuitry and radiating patches in hybrid or monolithic integrated circuit technologies.

These potential advantages with the steady interest in high frequency bands lead to the need for accurate analysis of such structures with very general bianisotropic substrates. The analysis and the solution of the electromagnetic field problem becomes simpler if the Fourier transformed domain- or spectral domain- approach is used. This is mainly due to the fact that Green's function convolution integrals in the spectral domain are turned into algebraic products. Different methods utilizing conventional spectral domain approaches have been proposed for the analysis of planar layered structures. Among those, there are the quasi static approaches and the full wave solutions [6].

A large number of works can be found in the literature dealing with the full wave solutions, all of which emphasize certain aspects but are restricted to either lossless substrates and/or conductors, infinitely thin conductors, magnetic bias in only one direction, purely diagonal constitutive tensors, or single layered substrates. Although the method proposed by Krowne [7,8], the propagation matrix approach, appears to be general because it includes bianisotropic media, it lacks closed-form expressions for dyadic Green's function. As an alternative, a similar scheme, called equivalent boundary method, has been presented by Mesa [9,10] to derive a spectral dyadic Green's function under the assumption, however, of lossless.

In this paper a generalized spectral-domain approach based on the transverse transmission-line method is presented. Such a method, also called Immittance Matrix Approach (IMA), based upon the decomposition of the spectral electromagnetic field into transverse TE and TM modes to the vertical axis, is quite different from the propagation matrix approach and the equivalent boundary methods. The IMA, in fact, is able to deal with any number of layers with or without losses and leads to compact algorithm for computing, besides, the far field radiated pattern and very interesting conditions of radiation on the horizon plane.

Up to now, this method has been used for the study of all the configurations which provide directly for two decoupled equations relating together sources and fields, one for the transverse TE modes and

another for the transverse TM modes. This condition is satisfied, for instance, by isotropic and, uniaxial and gyrotropic anisotropic layers with their optical axes perpendicular to the interface.

The theoretical formulation presented in this paper shows how to determine, via the Immittance Matrix Approach, the spectral dyadic Green's function of a single layered planar structure having a complex bianisotropic slab, fed by a planar electric point-source. To this end, firstly, we show how to decouple in a general unbounded bianisotropic medium the Maxwell's equations in spectral TE and TM waves with respect to the direction perpendicular to the interface. Secondly, we provide the conditions that must be satisfied by the constitutive tensors of the medium in order to describe, in the two-dimensional Fourier domain, the electromagnetic field via the transmission-line analogy. Starting from the transmission-line representation of the TE and TM spectral waves we, then, derive a general and very simple expression of the spectral Green's dyad for the single layered planar structure.

The method is demonstrated at the examples of a new synthetic bianisotropic material, recently introduced by Engheta and Saadoun: the pseudochiral Ω-medium [11–15]. There are four major mechanisms of producing the dipole moment in a material (the electronic, atomic, dipole and interfacial polarization). The electronic polarization is caused by a slight displacement of electrons surrounding positively charged atomic nuclei under the influence of the local electric field $\mathbf{E}'$, forming a dipole. The atomic polarization is caused by displacement of differently charged atoms with respect to each other. The dipole polarization, also called the orientation polarization, is caused by the change of the orientation of equivalent dipoles in a medium. These three kinds of polarizations are due to the locally bound charges in the atoms or molecules. The fourth polarization is called the space charge or interfacial polarization. Examples of the fourth polarization are provided by the chiral and pseudochiral materials. The pseudochiral medium is an artificial material which is obtained by diffusion of planar conducting microstructures, having the shape of Ω, into an isotropic dielectric medium. In order to treat the homogeneous mixture, electromagnetic scattering effects are not allowed, so the size of the inclusion has to be smaller than the wavelength of the operating field. The resulting macroscopic permittivity, permeability and pseudochirality admittance can be seen as a generalization of the Maxwell-Garnett mixing formula for heterogeneous dielectrics. The Ω-shaped conducting microstructures,

inside the host dielectric medium, increase the coupling of electric and magnetic fields as it happens with chiral media. The Ω-medium differs from the chiral one, and for this reason it is referred as pseudochiral [11], both because the Ω-shaped microstructures are not chiral geometric entities, since they can be superimposed on their specular (mirror) images, and because the induced electric and magnetic dipoles are mutually orthogonal. The induction in the host dielectric medium of an electric dipole and a magnetic one mutually orthogonal is the distinctive feature of Ω-medium. The orthogonality among these dipoles also implies that the orientation of the doping elements into the host isotropic medium cannot be random but must be parallel to a unique preferred direction. In fact, with a random distribution of conducting microstructures the total magnetoelectric coupling will result in a null average. Therefore, the pseudochiral Ω-medium is a particular bianisotropic medium.

Finally, the expression of the electric field radiated by a pseudochiral grounded slab is given. The expression of the radiated electric field is such as to simplify the extraction of important information to be used during the project, about the influence of frequency, constitutive parameters, thickness of the slab, position of the electric source, and, in particular, it is such as to obtain a nice condition of radiation on the horizon plane. Eventually, we remark that, once the modelization of the considered bianisotropic medium is deduced through the transmission-line analogy, the number of iso/bianisotropic dielectric layers is no longer an obstacle for the analysis.

2. Full Wave Analysis

In this Section we consider the formulation of the electromagnetic problem in a general bianisotropic medium, the decoupling of the differential equations describing the electromagnetic field and the formalization of the electromagnetic problem in the pseudochiral medium.

2.1 Formulation of the Electromagnetic Problem in a General Bianisotropic Medium

Let us consider an unbounded space filled with a general, linear, bianisotropic material described by four three-dimensional tensors $\underline{\epsilon}, \underline{\Omega}_{em}, \underline{\Omega}_{me}, \underline{\mu}$ and by the constitutive relations [13]:

$$\begin{cases} \mathbf{D} = \underline{\epsilon} \cdot \mathbf{E} + \underline{\Omega}_{em} \cdot \mathbf{B} \\ \mathbf{H} = \underline{\Omega}_{me} \cdot \mathbf{E} + \underline{\mu}^{-1} \cdot \mathbf{B} \end{cases} \tag{1a}$$

The constitutive relations (1) can also be expressed in the form of $\mathbf{D}$ and $\mathbf{B}$ as a function of $\mathbf{E}$ and $\mathbf{H}$:

$$\begin{cases} \mathbf{D} = \underline{\epsilon} \cdot \mathbf{E} + \underline{\sigma} \cdot \mathbf{H} \\ \mathbf{H} = \underline{\tau} \cdot \mathbf{E} + \underline{\mu} \cdot \mathbf{H} \end{cases} \tag{1b}$$

where $\underline{\sigma} = \underline{\Omega}_{em} \cdot \underline{\mu}$ and $\underline{\tau} = -\underline{\mu} \cdot \underline{\Omega}_{me}$

Under time harmonic excitations (e^{jwt}), the generic entry of the four constitutive tensors may be a complex quantity. Not all the entries of the constitutive tensors are necessarily non zero. From considerations of energy conservation [16,17], it can be proved that, for non-dissipative materials, the entries of $\underline{\epsilon}, \underline{\Omega}_{em}, \underline{\Omega}_{me}, \underline{\mu}$ must satisfy the following symmetry conditions:

$$\begin{cases} \underline{\epsilon} = \underline{\epsilon}^{+} \\ \underline{\mu} = \underline{\mu}^{+} \\ \underline{\Omega}_{me} = -\underline{\Omega}_{em}^{+} \end{cases} \tag{2}$$

where superscript + denotes transpose and complex conjugate.

The time harmonic Maxwell's equations in presence of electric $\mathbf{J}$ and magnetic $\mathbf{M}$ sources are:

$$\begin{cases} \nabla \times \mathbf{E} = -j\omega\mathbf{B} - \mathbf{M} \\ \nabla \times \mathbf{H} = j\omega\mathbf{D} + \mathbf{J} \end{cases} \tag{3}$$

In this part of the subsection, we do not restrict ourselves to any particular bianisotropic medium. The Full Wave Analysis based on the Immittance Matrix Approach will be generalized to the study of bianisotropic media. The spectral domain Immittance Matrix Approach is based on the two-dimensional Fourier transform defined by:

$$\begin{cases} \tilde{\Psi}(\alpha, y, \beta) = \displaystyle\int_{-\infty}^{+\infty} \int_{-\infty}^{+\infty} \Psi(x, y, z) e^{j(\alpha x + \beta z)}\, dx\, dz \\ \Psi(x, y, z) = \dfrac{1}{4\pi^2} \displaystyle\int_{-\infty}^{+\infty} \int_{-\infty}^{+\infty} \tilde{\Psi}(\alpha, y, \beta) e^{-j(\alpha x + \beta z)}\, d\alpha\, d\beta \end{cases} \tag{4}$$

By changing the Cartesian coordinate system $\Omega(x,y,z)$ into the associated one $\Omega(v,y,u)$ defined by the matrix $\underline{\mathbf{T}}$:

$$\begin{bmatrix} A_v \\ A_y \\ A_u \end{bmatrix} = \begin{bmatrix} \sin(\delta) & 0 & \cos(\delta) \\ 0 & 1 & 0 \\ -\cos(\delta) & 0 & \sin(\delta) \end{bmatrix} \begin{bmatrix} A_x \\ A_y \\ A_z \end{bmatrix} = \underline{\mathbf{T}} \cdot \begin{bmatrix} A_x \\ A_y \\ A_z \end{bmatrix} \qquad (5)$$

$$\text{with} \begin{cases} \alpha = \xi \sin(\delta) \\ \beta = \xi \cos(\delta) \end{cases}$$

in the spectral domain defined by (4), the Maxwell's equations become:

$$\begin{cases} \dfrac{\partial \tilde{E}_u}{\partial y} = -j\omega \tilde{B}_v \\ \dfrac{\partial \tilde{E}_v}{\partial y} = j\omega \tilde{B}_u + j\xi \tilde{E}_y \\ \dfrac{\partial \tilde{H}_u}{\partial y} = j\omega \tilde{D}_v \\ \dfrac{\partial \tilde{H}_v}{\partial y} = -j\omega \tilde{D}_u + j\xi \tilde{H}_y \\ \tilde{B}_y = \dfrac{\xi}{\omega} \tilde{E}_u \\ \tilde{D}_y = -\dfrac{\xi}{\omega} \tilde{H}_u \end{cases} \qquad (6)$$

By using the constitutive relations we derive:

1) two linear relations among the longitudinal components and the transverse ones of the spectral electromagnetic field:

$$\begin{cases} \tilde{E}_y = f_1(\xi, \tilde{E}_v, \tilde{E}_u, \tilde{H}_v, \tilde{H}_u) \\ \tilde{H}_y = f_2(\xi, \tilde{E}_v, \tilde{E}_u, \tilde{H}_v, \tilde{H}_u) \end{cases} \qquad (7)$$

2) the subsystem of partial differential equations describing the transverse spectral electromagnetic field:

$$\begin{cases} \dfrac{\partial \mathbf{V}}{\partial y} = -\underline{\mathbf{C}}_{VI} \cdot \mathbf{I} - \underline{\mathbf{C}}_{VV} \cdot \mathbf{V} \\ \dfrac{\partial \mathbf{I}}{\partial y} = -\underline{\mathbf{C}}_{II} \cdot \mathbf{I} - \underline{\mathbf{C}}_{IV} \cdot \mathbf{V} \end{cases} \qquad (8)$$

with

$$\mathbf{V} = \begin{bmatrix} \tilde{E}_v \\ \tilde{E}_u \end{bmatrix} \qquad \mathbf{I} = \begin{bmatrix} \tilde{H}_u \\ \tilde{H}_v \end{bmatrix} \tag{9a}$$

The matrices $\underline{\mathbf{C}}_{VI}, \underline{\mathbf{C}}_{VV}, \underline{\mathbf{C}}_{IV}, \underline{\mathbf{C}}_{II}$ are the entries of the supermatrix $\underline{\mathbf{C}}$ so defined:

$$\mathbf{C} = \begin{bmatrix} \underline{\mathbf{C}}_{VI} & \underline{\mathbf{C}}_{VV} \\ \underline{\mathbf{C}}_{II} & \underline{\mathbf{C}}_{IV} \end{bmatrix} = \begin{bmatrix} \begin{bmatrix} c_{11} & c_{12} \\ c_{21} & c_{22} \end{bmatrix} & \begin{bmatrix} c_{13} & c_{14} \\ c_{23} & c_{24} \end{bmatrix} \\ \begin{bmatrix} c_{31} & c_{32} \\ c_{41} & c_{42} \end{bmatrix} & \begin{bmatrix} c_{33} & c_{34} \\ c_{43} & c_{44} \end{bmatrix} \end{bmatrix} \tag{9b}$$

and the formal expressions of $c_{ij}(i,j = 1,2,3,4)$ are reported in Appendix.

In general, $\underline{\mathbf{C}}$ has sixteen elements. Therefore, system (8) represents a set of partial differential equations of the first order (coupled transverse transmission-line equations) and shows a coupling between the $\mathbf{V}$ and $\mathbf{I}$ vectors. System (8) can be decoupled when:

$$\begin{cases} \underline{\mathbf{C}}_{VV} = 0 \\ \underline{\mathbf{C}}_{II} = 0 \end{cases} \tag{10}$$

When (10) holds, relations (7) and (8) become, respectively:

$$\begin{cases} \tilde{E}_y = -\dfrac{\xi + \omega\sigma_{yu}}{\omega\epsilon_{yy}}\tilde{H}_u - \dfrac{\sigma_{yv}}{\epsilon_{yy}}\tilde{H}_v \\ \tilde{H}_y = \dfrac{\xi - \omega\tau_{yu}}{\omega\mu_{yy}}\tilde{E}_u - \dfrac{\tau_{yv}}{\mu_{yy}}\tilde{E}_v \end{cases} \tag{11a}$$

and

$$\begin{cases} \dfrac{\partial \mathbf{V}}{\partial y} = -\underline{\mathbf{C}}_{VI} \cdot \mathbf{I} \\ \dfrac{\partial \mathbf{I}}{\partial y} = -\underline{\mathbf{C}}_{IV} \cdot \mathbf{V} \end{cases} \tag{11b}$$

where σ_{ij} and $\tau_{ij}(i,j = v,y,u)$ are the entries of the matrices σ and τ in the new reference system $\Omega(v,y,u)$. By virtue of (10), it can be established that the decoupling between $\mathbf{V}$ and $\mathbf{I}$ is always satisfied when the constitutive tensors are of the form:

$$
\begin{aligned}
\underline{\epsilon} &= \begin{bmatrix} \epsilon_{xx} & 0 & \epsilon_{xz} \\ 0 & \epsilon_{yy} & 0 \\ \epsilon_{zx} & 0 & \epsilon_{zz} \end{bmatrix} \\
\underline{\Omega}_{em} &= \begin{bmatrix} 0 & \Omega_{xy}^{(em)} & 0 \\ \Omega_{yx}^{(em)} & 0 & \Omega_{yz}^{(em)} \\ 0 & \Omega_{zy}^{(em)} & 0 \end{bmatrix} \\
\underline{\Omega}_{me} &= \begin{bmatrix} 0 & \Omega_{xy}^{(me)} & 0 \\ \Omega_{yx}^{(me)} & 0 & \Omega_{yz}^{(me)} \\ 0 & \Omega_{zy}^{(me)} & 0 \end{bmatrix} \\
\underline{\mu} &= \begin{bmatrix} \mu_{xx} & 0 & \mu_{xz} \\ 0 & \mu_{yy} & 0 \\ \mu_{zx} & 0 & \mu_{zz} \end{bmatrix}
\end{aligned}
\tag{12}
$$

From (2) and (12), Ω_{me} is completely determined by Ω_{em}. Tensors $\underline{\epsilon}$ and $\underline{\mu}$ are Hermitian; when they are real, they are symmetrical. $\underline{\epsilon}$ and $\underline{\mu}$ are made of four independent elements. In general, Ω_{em} has four elements. Therefore, in order to decouple the Maxwell's equations in the spectral domain, the constitutive tensors have to contain a total of 12 independent elements.

2.2 Decoupling of the Differential Equations Describing the Electromagnetic Field.

Equations (11.b) are two coupled first-order vector differential equations for the two field quantities $\mathbf{V}$ and $\mathbf{I}$. We can combine these two equations, eliminate one of the field quantities and obtain the uncoupled second-order vector differential equations for one field quantity:

$$
\begin{cases}
\dfrac{\partial^2 \mathbf{V}}{\partial y^2} = \underline{\mathbf{C}}_{VI} \cdot \underline{\mathbf{C}}_{IV} \cdot \mathbf{V} = \underline{\mathbf{D}}^{zy} \cdot \mathbf{V} \\
\dfrac{\partial^2 \mathbf{I}}{\partial y^2} = \underline{\mathbf{C}}_{IV} \cdot \underline{\mathbf{C}}_{VI} \cdot \mathbf{I} = \underline{\mathbf{D}}^{yz} \cdot \mathbf{I}
\end{cases}
\tag{13}
$$

The eigenvectors $\mathbf{V}$ and $\mathbf{I}$ are of the form:

$$\begin{cases} \mathbf{V}(\alpha, y, \beta) = \mathbf{V}(\alpha, \beta) e^{k_y y} \\ \mathbf{I}(\alpha, y, \beta) = \mathbf{I}(\alpha, \beta) e^{k_y y} \end{cases} \tag{14}$$

The spectral wavenumbers k_y are the eigenvalues of $\mathbf{D}^{ZY}$ or, equivalently, $\mathbf{D}^{YZ}$. The dispersion relation satisfied by the spectral wavenumber is:

$$\det\left[k_y^2 \underline{\mathbf{U}} - \underline{\mathbf{D}}^{ZY}\right] = \det\left[k_y^2 \underline{\mathbf{U}} - \underline{\mathbf{D}}^{YZ}\right] = 0 \tag{15}$$

where $\underline{\mathbf{U}}$ is the unity matrix. The solutions of (15) point out the existence of a double mode of propagation that we associate to an ordinary $(k_y^{(o)})$ and to an extraordinary $(k_y^{(e)})$ vertical wavenumber defined by:

$$\begin{cases} k_y^{(o)} = \pm\sqrt{\dfrac{D_{11}^{ZY} + D_{22}^{ZY} + \sqrt{(D_{11}^{ZY} - D_{22}^{ZY})^2 + 4D_{12}^{ZY} D_{21}^{ZY}}}{2}} \\ k_y^{(e)} = \pm\sqrt{\dfrac{D_{11}^{ZY} + D_{22}^{ZY} - \sqrt{(D_{11}^{ZY} - D_{22}^{ZY})^2 + 4D_{12}^{ZY} D_{21}^{ZY}}}{2}} \end{cases} \tag{16}$$

The relations of proportionality among the components of the eigenvectors $\mathbf{V}(\alpha, \beta)$ and $\mathbf{I}(\alpha, \beta)$ have a double determination related to the expressions of the two eigenmodes of propagation:

$$\begin{cases} \dfrac{\tilde{E}_u^{(o,e)}}{\tilde{E}_v^{(o,e)}} = \Psi_e^{(o,e)} = \dfrac{M_{ZY} \pm \sqrt{M_{ZY}^2 + 4P_{ZY}}}{2D_{12}^{ZY}} \\ \dfrac{\tilde{H}_u^{(o,e)}}{\tilde{H}_v^{(o,e)}} = \Psi_h^{(o,e)} = \dfrac{2D_{12}^{ZY}}{M_{ZY} \pm \sqrt{M_{YZ}^2 + 4P_{YZ}}} \end{cases} \tag{17}$$

with

$$\begin{cases} M_{(ZY,YZ)} = D_{11}^{(ZY,YZ)} - D_{22}^{(ZY,YZ)} \\ P_{(ZY,YZ)} = D_{12}^{(ZY,YZ)} D_{21}^{(ZY,YZ)} \end{cases} \tag{18}$$

By virtue of (17), the spectral electromagnetic field can be decomposed into two sets of $\mathbf{TE}(\hat{y})$ and $\mathbf{TM}(\hat{y})$ waves different for the two eigenmodes, whose transverse components satisfy transmission-line equations.

TE$(\hat{y})$ waves satisfied by $\tilde{H}_v, \tilde{H}_y, \tilde{E}_u$

$$\begin{cases} \dfrac{\partial \tilde{E}_u^{(o,e)}}{\partial y} = -\left[c_{21}\Psi_h^{(o,e)} + c_{22}\right]\tilde{H}_v^{(o,e)} = -Z_{TE}^{(o,e)}\tilde{H}_v^{(o,e)} \\ \dfrac{\partial \tilde{H}_v^{(o,e)}}{\partial y} = -\left[\dfrac{c_{43} + c_{44}\Psi_e^{(o,e)}}{\Psi_e^{(o,e)}}\right]\tilde{E}_u^{(o,e)} = -Y_{TE}^{(o,e)}\tilde{E}_u^{(o,e)} \\ \tilde{H}_y^{(o,e)} = Y_y\,\tilde{E}_u^{(o,e)} \end{cases} \tag{19}$$

TM$(\hat{y})$ waves satisfied by $\tilde{E}_v, \tilde{E}_y, \tilde{H}_u$

$$\begin{cases} \dfrac{\partial \tilde{E}_v^{(o,e)}}{\partial y} = -\left[\dfrac{c_{11}\Psi_h^{(o,e)} + c_{12}}{\Psi_h^{(o,e)}}\right]\tilde{H}_u^{(o,e)} = -Z_{TM}^{(o,e)}\tilde{H}_u^{(o,e)} \\ \dfrac{\partial \tilde{H}_u^{(o,e)}}{\partial y} = -\left[c_{33} + c_{34}\Psi_e^{(o,e)}\right]\tilde{E}_v^{(o,e)} = -Y_{TM}^{(o,e)}\tilde{E}_v^{(o,e)} \\ \tilde{E}_y^{(o,e)} = Z_y\,\tilde{H}_u^{(o,e)} \end{cases} \tag{20}$$

The transmission lines are characterized, respectively, by the spectral wavenumbers along $\hat{y}\,k_y^{(o,e)}$ given by (16) and by the characteristic impedances:

$$\begin{cases} \eta_{TE}^{(o,e)} = \sqrt{\dfrac{Z_{TE}^{(o,e)}}{Y_{TE}^{(o,e)}}} \equiv \dfrac{j\omega\mu_0\mu_{vv}}{\delta_{TE}^{(o,e)}} \\ \eta_{TM}^{(o,e)} = \sqrt{\dfrac{Z_{TM}^{(o,e)}}{Y_{TM}^{(o,e)}}} \equiv \dfrac{\delta_{TE}^{(o,e)}}{j\omega\epsilon_0\epsilon_{vv}} \end{cases} \tag{21}$$

2.3 Formalization of the Electromagnetic Problem in the Pseudochiral Medium.

In this subsection we consider a pseudochiral medium in which the conducting microstructures are oriented as in Fig. 2.3.1.

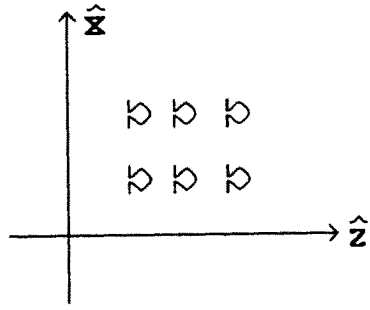

Figure 2.3.1 Spatial orientation of planar, Ω-shaped conducting microstructures in the hosting isotropic material.

In such media a time varying electric field, polarized along the $\hat{x}$-axis, originates not only an electric dipole but also, due to the presence of the conducting microstructures, a magnetic one directed along the $\hat{y}$-axis. Similarly, a time dependent magnetic field polarized along the $\hat{y}$-axis produces a magnetic dipole and induces an electric one directed as the $\hat{x}$-axis. It is easy to demonstrate that the constitutive relations of this Ω-medium are:

$$\begin{cases} \mathbf{D} = \underline{\epsilon} \cdot \mathbf{E} + \underline{\Omega}_{em} \cdot \mathbf{B} \\ \mathbf{H} = \underline{\Omega}_{me} \cdot \mathbf{E} + \mu^{-1} \cdot \mathbf{B} \end{cases} \tag{22}$$

with

$$\underline{\epsilon} = \begin{bmatrix} \epsilon_{xx} & 0 & 0 \\ 0 & \epsilon_{yy} & 0 \\ 0 & 0 & \epsilon_{zz} \end{bmatrix}$$

$$\underline{\Omega}_{em} = \begin{bmatrix} 0 & j\Omega_c & 0 \\ 0 & 0 & 0 \\ 0 & 0 & 0 \end{bmatrix} \qquad (23)$$

$$\underline{\Omega}_{me} = \begin{bmatrix} 0 & 0 & 0 \\ j\Omega_c & 0 & 0 \\ 0 & 0 & 0 \end{bmatrix}$$

$$\underline{\mu} = \begin{bmatrix} \mu_{xx} & 0 & 0 \\ 0 & \mu_{yy} & 0 \\ 0 & 0 & \mu_{zz} \end{bmatrix}$$

Note that the constitutive tensors of a pseudochiral medium are a particular determination of (12). By specifying (9.b) with the constitutive tensors of the pseudochiral medium (23), the supermatrix $\underline{\mathbf{C}}$ becomes:

$$\underline{C} = \begin{bmatrix} \underline{C}_{vI} & 0 \\ 0 & \underline{C}_{Iv} \end{bmatrix} \qquad (24)$$

where

$$\underline{C}_{vI} = e^{-j\frac{\pi}{2}} \cdot \begin{bmatrix} \frac{\xi^2 - \omega^2 \mu_{uu}\epsilon_{yy}}{\omega\epsilon_{yy}} & -\omega\mu_{uv} \\ \omega\mu_{uv} & \omega\mu_{vv} \end{bmatrix} \qquad (25a)$$

$$\underline{C}_{Iv} = e^{j\frac{\pi}{2}} \cdot \begin{bmatrix} \omega\epsilon_{vv} & \omega\epsilon_{uv} + j\xi\Omega_c \sin(\delta) \\ -\omega\epsilon_{uv} + j\xi\Omega_c \sin(\delta) & \frac{\xi^2 - \omega^2 \mu_{yy}\epsilon_{uu}}{\omega\mu_{yy}} \end{bmatrix} \qquad (25b)$$

$\epsilon_{ij}, \mu_{ij} (i, j = v, y, u)$ are the entries of $\underline{\epsilon}$ and $\underline{\mu}$ in the reference system $\Omega(v, y, u)$ related to the corresponding ones of e and m in the reference system $\Omega(x, y, z)$ through a linear transformation defined by the $\underline{\mathbf{T}}$ matrix:

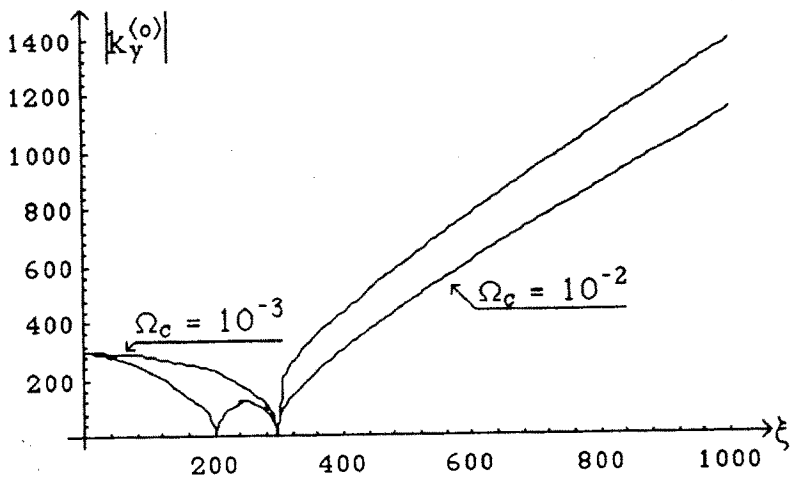

Figure 2.3.2 $\left|k_y^{(o)}\right|$ **as a function of the spectral wavenumber** ξ. $(\epsilon_{xx} = 4\epsilon_0, \epsilon_{yy} = \epsilon_{zz} = 2\epsilon_0, \mu_{xx} = \mu_{zz} = \mu_0, \mu_{yy} = 2\mu_0, f = 10\ \text{GHz}, \delta = \frac{\pi}{4})$.

$$
\begin{aligned}
\epsilon_{cc} &= \epsilon_{xx} + \mu_{yy}\Omega_c^2 \\
\epsilon_{vv} &= \epsilon_{xx}\sin^2(\delta) + \epsilon_{zz}\cos^2(\delta) \\
\epsilon_{uv} &= \epsilon_{vu} = (\epsilon_{zz} - \epsilon_{cc})\sin(\delta)\cos(\delta) \\
\epsilon_{uu} &= \epsilon_{xx}\cos^2(\delta) + \epsilon_{zz}\sin^2(\delta) \\
\sigma_{vy} &= j\mu_{yy}\Omega_c\sin(\delta) \\
\sigma_{uy} &= -j\mu_{yy}\Omega_c\cos(\delta) \\
\tau_{yv} &= -j\mu_{yy}\Omega_c\sin(\delta) \\
\tau_{yu} &= j\mu_{yy}\Omega_c\cos(\delta) \\
\mu_{vv} &= \mu_{xx}\sin^2(\delta) + \mu_{zz}\cos^2(\delta) \\
\mu_{uv} &= \mu_{vu} = (\mu_{zz} - \mu_{xx})\sin(\delta)\cos(\delta) \\
\mu_{uu} &= \mu_{xx}\cos^2(\delta) + \mu_{zz}\sin^2(\delta)
\end{aligned}
$$

As expected, due to the particular form of the constitutive tensors, matrix $\underline{\mathbf{C}}$ is in a block diagonal form and, then, the spectral elec-

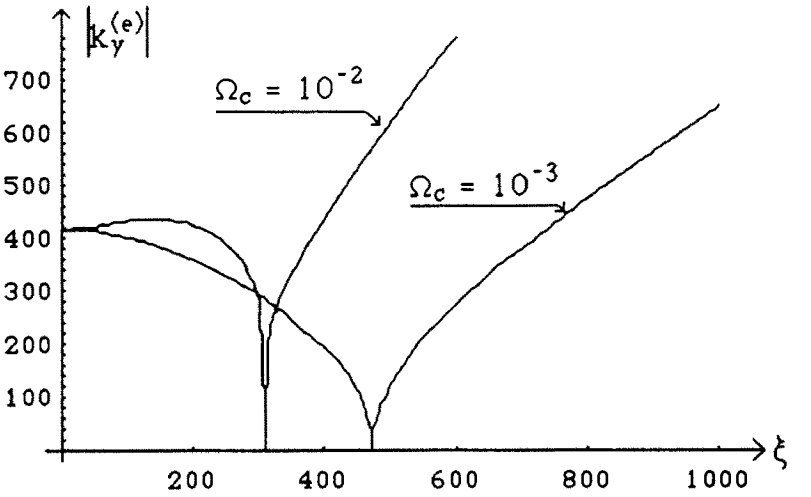

Figure 2.3.3 $\left|k_y^{(e)}\right|$ **as a function of the spectral wavenumber** ξ. $(\epsilon_{xx} = 4\epsilon_0, \epsilon_{yy} = \epsilon_{zz} = 2\epsilon_0, \mu_{xx} = \mu_{zz} = \mu_0, \mu_{yy} = 2\mu_0, f = 10$ **GHz**$, \delta = \frac{\pi}{4})$.

tromagnetic field in a pseudochiral medium can be decomposed into two spectra of $\mathbf{TE}(\hat{y})$ and $\mathbf{TM}(\hat{y})$ waves. In this case the vertical wavenumbers for the ordinary and extraordinary waves are given by:

$$k_y^{(o,e)} = \pm\sqrt{\frac{-d_2 \pm \sqrt{d_2^2 - 4d_4 d_0}}{2d_4}} \tag{26}$$

In (26) we have:

$$\begin{cases} d_4 = \epsilon_{yy}\mu_{yy} \\ d_2 = -s_{vv}\xi^2 + \epsilon_{yy}\mu_{yy}s_{xx}\omega^2 \\ d_0 = \epsilon_{cv}\mu_{vv}\xi^4 + \epsilon_{xx}\epsilon_{yy}\epsilon_{zz}\mu_{xx}\mu_{yy}\mu_{zz}\omega^4 \\ \qquad - (\epsilon_{xx}\epsilon_{zz}\mu_{vv}\mu_{yy} + \epsilon_{cv}\epsilon_{yy}\mu_{xx}\mu_{zz})\omega^2\xi^2 \\ \epsilon_{cv} = \epsilon_{vv} + \mu_{yy}\Omega_c^2\sin^2(\delta) \\ s_{ij} = \epsilon_{ii}\mu_{jj} + \epsilon_{jj}\mu_{ii} \\ d_{ij} = \epsilon_{ii}\mu_{jj} - \epsilon_{jj}\mu_{ii} \qquad (i,j = x,v,y,z,u) \end{cases} \tag{27}$$

In contrast of the isotropic and bi-isotropic case [18,19] and like the anisotropic one [20], the vertical wavenumbers in a pseudochiral medium are function not only on ξ but also on δ. The behaviors of vertical wavenumbers for the ordinary and extraordinary waves, for a particular cut in δ, are shown in Fig. 2.3.2 and Fig. 2.3.3.

In the $\alpha-\beta$ plane the zeros of $k_y^{(o)}$ lie into two ellipses defined by:

$$\frac{\alpha^2}{\omega^2 \frac{\epsilon_{xx}}{\epsilon_{cc}} \epsilon_{xx}\mu_{yy}} + \frac{\beta^2}{\omega^2 \epsilon_{xx}\mu_{yy}} = 1 \tag{28a}$$

$$\frac{\alpha^2}{\omega^2 \epsilon_{yy}\mu_{zz}} + \frac{\beta^2}{\omega^2 \epsilon_{yy}\mu_{xx}} = 1 \tag{28b}$$

The zeros of $k_y^{(e)}$, if there, are the solution of the following two systems:

$$\begin{cases} \dfrac{\alpha^2}{\omega^2 \epsilon_{xx}\mu_{yy} \frac{\epsilon_{xx}}{\epsilon_{cc}}} + \dfrac{\beta^2}{\omega^2 \epsilon_{xx}\mu_{yy}} = 1 \\ \dfrac{\alpha^2 s_{xy}}{\omega^2 \epsilon_{yy}\mu_{yy} s_{xz}} + \dfrac{\beta^2 s_{yz}}{\omega^2 \epsilon_{yy}\mu_{yy} s_{xz}} = 1 \end{cases} \tag{29}$$

$$\begin{cases} \dfrac{\alpha^2}{\omega^2 \epsilon_{yy}\mu_{zz}} + \dfrac{\beta^2}{\omega^2 \epsilon_{yy}\mu_{xx}} = 1 \\ \dfrac{\alpha^2 s_{xy}}{\omega^2 \epsilon_{yy}\mu_{yy} s_{xz}} + \dfrac{\beta^2 s_{yz}}{\omega^2 \epsilon_{yy}\mu_{yy} s_{xz}} = 1 \end{cases} \tag{30}$$

Therefore, the zeros of $k_y^{(e)}$ are given by the intersections of the ellipses (28a) and (28b) with the ellipse

$$\frac{\alpha^2 s_{xy}}{\omega^2 \epsilon_{yy}\mu_{yy} s_{xz}} + \frac{\beta^2 s_{yz}}{\omega^2 \epsilon_{yy}\mu_{yy} s_{xz}} = 1$$

When some specific conditions are imposed on the electromagnetic parameters, for the corresponding values of α and β, the discriminant of (26) vanishes. In this case the wavenumbers of the ordinary and extraordinary waves are the same. Thus, we are in a monomodality regime. This means that the Ω-medium suffers only an ordinary wave. The condition that must be satisfied by the electromagnetic parameters and the wavenumbers α, β to obtain the monomodal regime of propagation along the $\widehat{y}$-direction is:

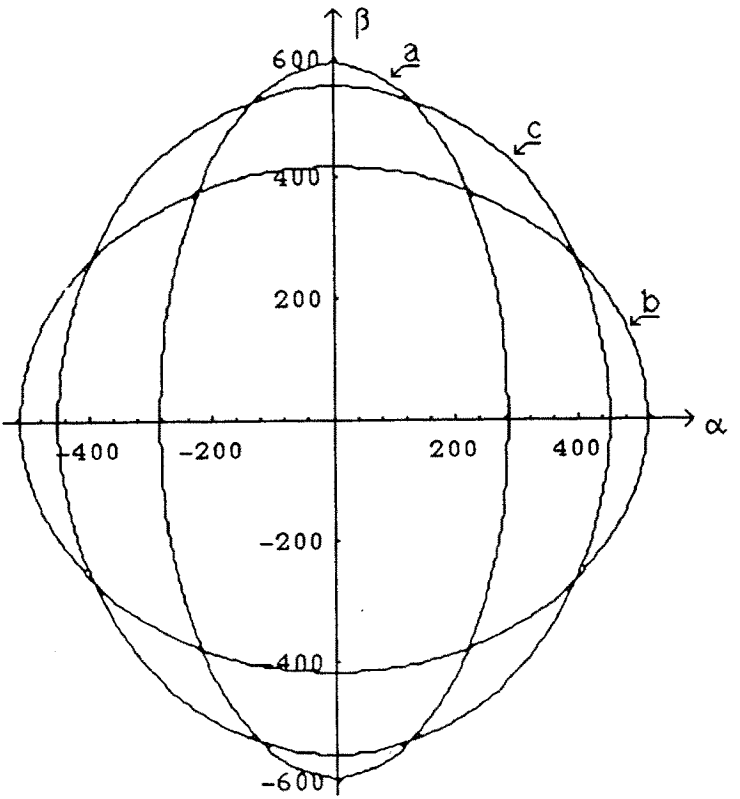

Figure 2.3.4 a,b) Loci $k_y^{(o)} = 0$; **c)** ellipse $\frac{\alpha^2 s_{xy}}{\omega^2 \epsilon_{yy}\mu_{yy}s_{xz}} + \frac{\beta^2 s_{yz}}{\omega^2 \epsilon_{yy}\mu_{yy}s_{xz}} = 1$; $(\epsilon_{xx} = 4\epsilon_0, \epsilon_{yy} = 2\epsilon_0, \epsilon_{zz} = \epsilon_0, \mu_{xx} = \mu_{yy} = 2\mu_0, \mu_{zz} = 3\mu_0, f = 10$ **GHz**, $\Omega_c = 10^{-3}\Omega^{-1}$).

$$
\begin{aligned}
&(d_{xy}^2 - 4\epsilon_{yy}\mu_{xx}\mu_{yy}^2\Omega_c^2)\alpha^4 + d_{yz}^2\beta^4 - 2(d_{xy}d_{yz} + 2\epsilon_{yy}\mu_{zz}\mu_{yy}^2\Omega_c^2)\alpha^2\beta^2 \\
&\quad -2\epsilon_{yy}\mu_{yy}\omega^2[s_{xy}s_{xz} - 2\mu_{xx}(\epsilon_{xx}s_{yz} + \epsilon_{yy}\mu_{yy}\mu_{zz}\Omega_c^2)]\alpha^2 \\
&\quad -2\epsilon_{yy}\mu_{yy}\omega^2(s_{xz}s_{yz} - 2\epsilon_{zz}\mu_{zz}s_{xy})\beta^2 + d_{xz}^2\epsilon_{yy}^2\mu_{yy}^2\omega^4 = 0
\end{aligned}
\tag{31}
$$

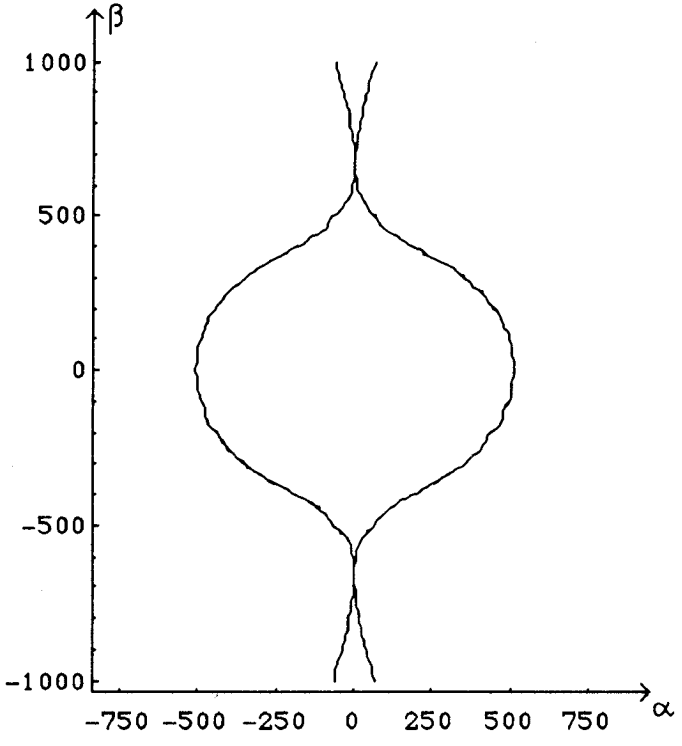

Figure 2.3.5 Locus of monomodality $(k_y^{(o)} = k_y^{(e)})$ **in the** $\alpha - \beta$ **plane** $(\epsilon_{xx} = 4\epsilon_0, \epsilon_{yy} = 2\epsilon_0, \epsilon_{zz} = \epsilon_0, \mu_{xx} = \mu_{yy} = 2\mu_0, \mu_{zz} = 3\mu_0, f = 10$ **GHz**, $\Omega_c = 10^{-3}\Omega^{-1})$.

In Fig. 2.3.5 is shown the behavior of the locus of monomodality in the $\alpha - \beta$ plane.

Both the propagation and the polarization of the spatial electromagnetic field are affected by the spectral wavenumbers $k_y^{(0,e)}$ of the ordinary and extraordinary waves. In fact, the i-th component of the spatial electric (magnetic) field can be written in terms of its two-dimensional Fourier transform:

$$E_i(x,y,z) = \frac{1}{4\pi^2} \int_{-\infty}^{+\infty} \int_{-\infty}^{+\infty} \tilde{e}_i(\alpha,\beta) e^{-j\alpha x + k_y^{(0,e)}(\alpha,\beta) y - j\beta z} \, d\alpha \, d\beta \quad (32)$$

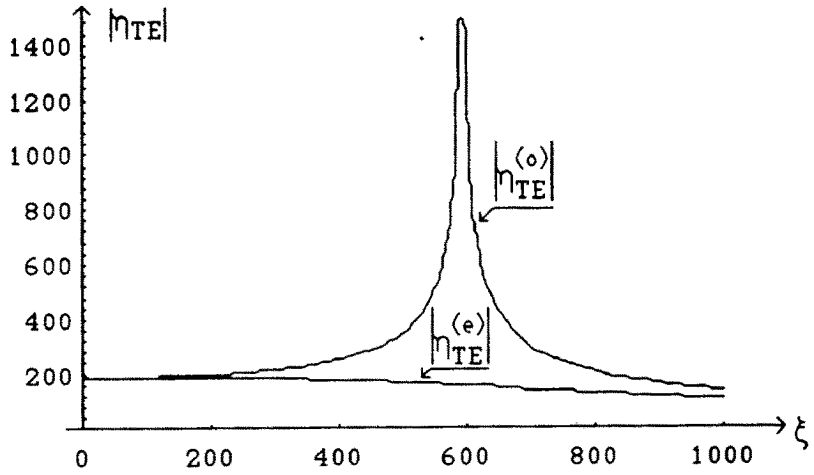

Figure 2.3.6 Modulus of the characteristic impedances for the ordinary and extraordinary TE($\widehat{y}$) waves. ($\epsilon_{xx} = 6\epsilon_0, \epsilon_{yy} = \epsilon_{zz} = 2\epsilon_0, \mu_{xx} = \mu_{zz} = \mu_0, \mu_{yy} = 2\mu_0, \Omega_c = 10^{-3}\Omega^{-1}, f = 10$ **GHz**, $\delta = \frac{\pi}{2}$).

When the spectral waves are confined to propagate in the $x-z$ plane, i.e. in the plane parallel to that containing the conducting microstructures, the spatial electric field is given by a superposition of linearly polarized waves. The generic component of the spectral field is circularly polarized when:

$$k_y^{(o,e)}(\alpha, \beta) = \xi^2 \tag{33}$$

The proportionality constants $\Psi_e(\alpha, \beta)$ and $\Psi_h(\alpha, \beta)$ can be evaluated directly, by specifying (17) with (23). From (19) and (20), once the proportionality constants $\Psi_e(\alpha, \beta)$ and $\Psi_h(\alpha, \beta)$ are known, it is easy to deduce the primary constants associated with the spectral transverse transmission lines and, then, the corresponding differential elements for each spectrum.

The behaviors of the spectral characteristics impedances are shown in Figs. 2.3.6–2.3.7.

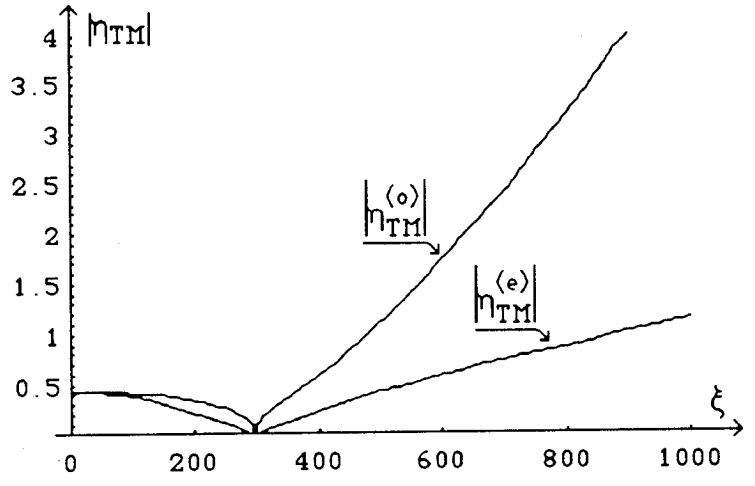

Figure 2.3.7 Modulus of the characteristic impedances for the ordinary and extraordinary TM($\widehat{y}$) waves ($\epsilon_{xx} = 6\epsilon_0, \epsilon_{yy} = \epsilon_{zz} = 2\epsilon_0, \mu_{xx} = \mu_{zz} = \mu_0, \mu_{yy} = 2\mu_0, \Omega_c = 10^{-3}\Omega^{-1}, f = 10$ **GHz**, $\delta = \frac{\pi}{2}$).

3. Pseudochiral Slab Embedded in an Isotropic Half-Space

In this Section we consider the spectral electric Green's dyad, the radiated electric field with some numerical examples for a pseudochiral grounded slab with a planar electric source.

3.1 Spectral Electric Green's Dyad

Let us consider a planar structure (Fig.3.1) formed by a grounded pseudochiral slab described by (23), in presence of an isotropic half-space, fed by a planar electric source inside the slab:

$$\mathbf{J} = [J_x(x, -h, z)\widehat{x} + J_z(x, -h, z)\widehat{z}]\, \delta_0(y + h) \tag{34}$$

where $\delta_0(y + h)$ is the Dirac function.

The elements of the first and third row of the spectral electric Green's dyad may be obtained in a straightforward manner by making

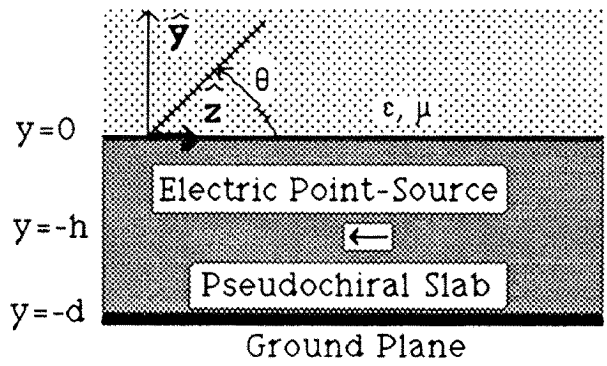

Figure 3.1 Planar pseudochiral slab fed by an electric point-source.

use of the equivalent transmission lines. To this end, in the previous sections we have decomposed in the two-dimensional Fourier domain all the field components as superposition of $\mathbf{TE}(\hat{y})$ and $\mathbf{TM}(\hat{y})$ waves and drawn equivalent circuits for the $\mathbf{TE}(\hat{y})$ and $\mathbf{TM}(\hat{y})$ fields:

$$\tilde{\mathbf{E}}(\alpha, y, \beta) = \int_{-\infty}^{+\infty} \underline{\tilde{\mathbf{G}}}(\alpha, y, \beta | y') \cdot \tilde{\mathbf{J}}(\alpha, y', \beta)\, dy' = \tilde{\mathbf{E}}_v^{TM} + \tilde{\mathbf{E}}_y^{TM} + \tilde{\mathbf{E}}_u^{TE} \tag{35}$$

Once the transmission line problems are solved, the final step of the formulation consists of the mapping from the $\Omega(v, y, u)$ coordinate system to the Cartesian one $\Omega(x, y, z)$. Because of the coordinate transform relation (5), $\tilde{\mathbf{E}}_x$ and $\tilde{\mathbf{E}}_z$ are linearly related to $\tilde{\mathbf{E}}_u$ and $\tilde{\mathbf{E}}_v$, Similarly, $\tilde{\mathbf{J}}_x$ and $\tilde{\mathbf{J}}_z$ are superposition of $\tilde{\mathbf{J}}_u$ and $\tilde{\mathbf{J}}_v$. When (5) is used, the elements of the first and third row of the spectral electric Green's dyad in each region are given by:

$$\begin{cases} \tilde{G}_{xx,k} = A_k^{TM}\dfrac{\alpha^2}{\alpha^2+\beta^2} - A_k^{TE}\dfrac{\beta^2}{\alpha^2+\beta^2} \\ \tilde{G}_{xz,k} = (A_k^{TM} + A_k^{TE})\dfrac{\alpha\beta}{\alpha^2+\beta^2} \\ \tilde{G}_{yx,k} = \dfrac{Z_{y,k}}{\eta_k^{TM}} A_k^{TM}\dfrac{\alpha}{\sqrt{\alpha^2+\beta^2}} \\ \tilde{G}_{yz,k} = \dfrac{Z_{y,k}}{\eta_k^{TM}} A_k^{TM}\dfrac{\beta}{\sqrt{\alpha^2+\beta^2}} \\ \tilde{G}_{zx,k} = \tilde{G}_{xz,k} \\ \tilde{G}_{zz,k} = A_k^{TM}\dfrac{\beta^2}{\alpha^2+\beta^2} - A_k^{TE}\dfrac{\alpha^2}{\alpha^2+\beta^2} \end{cases} \qquad (k=1,2,3) \tag{36}$$

where

$$\begin{cases} A_1^{(TE,TM)} = \eta_1^{(TE,TM)}\dfrac{F_1^{(TE,TM)}(h)}{F_1^{(TE,TM)}(d)}\sinh[k_y(d+y)] \\ A_2^{(TE,TM)} = \eta_1^{(TE,TM)}\dfrac{F_2^{(TE,TM)}(y)}{F_1^{(TE,TM)}(d)}\sinh[k_y(d-h)] \\ A_3^{(TE,TM)} = \eta_1^{(TE,TM)}\eta_2^{(TE,TM)}\dfrac{e^{-k_2 y}}{F_1^{(TE,TM)}(d)}\sinh[k_y(d+y)] \end{cases}$$

$$k_2 = \sqrt{\alpha^2+\beta^2-\omega^2\epsilon\mu}$$

$$\begin{cases} \eta_1^{TE} = \dfrac{j\omega\mu_{vv}}{\delta_{TE}} \\ \eta_1^{TM} = \dfrac{\delta_{TM}}{j\omega\epsilon_{vv}} \end{cases} \qquad \begin{cases} \eta_2^{TE} = \dfrac{j\omega\mu}{k_2} \\ \eta_2^{TM} = \dfrac{k_2}{j\omega\epsilon} \end{cases}$$

$$\begin{cases} Z_{y,1} = Z_{y,2} = -\dfrac{\sqrt{\alpha^2+\beta^2}}{\omega\epsilon_{yy}} \\ Z_{y,3} = -\dfrac{\sqrt{\alpha^2+\beta^2}}{\omega\epsilon} \end{cases}$$

$$\begin{cases} F_1^{(TE,TM)}(x) = \eta_2^{(TE,TM)} \cosh(k_y x) + \eta_1^{(TE,TM)} \sinh(k_y x) \\ F_2^{(TE,TM)}(y) = \eta_2^{(TE,TM)} \cosh(k_y y) - \eta_1^{(TE,TM)} \sinh(k_y y) \end{cases} \tag{37}$$

Six elements of the spectral electric Green's dyad for each one of the three regions into which the structure is divided have been determined. To complete the evaluation of the elements of the whole dyadic function it is necessary to determine the terms of the second column. The elements $\tilde{G}_{ij}(i = x, y, z; j = y)$ can be obtained via the reciprocity theorem appropriately modified for a bianisotropic medium:

$$\int_{V_1} \mathbf{J}_1 \cdot \mathbf{E}_2 \, dV_1 = \int_{V_2} \mathbf{J}_2 \cdot \mathbf{E}_1^{(c)} \, dV_2 \tag{38}$$

with V_1 = volume of source $\mathbf{J}_1$ and V_2 = volume of source $\mathbf{J}_2$. The so-called modified reciprocity theorem states that the reaction of source $\mathbf{J}_1$ caused by source $\mathbf{J}_2$ in a bianisotropic medium is equal to the reaction of source $\mathbf{J}_2$ caused by source $\mathbf{J}_1$ in the complementary medium. If a bianisotropic medium is characterized by the following constitutive relations [16]:

$$\begin{cases} \mathbf{B} = \underline{\zeta} \cdot \mathbf{E} + \underline{\mu} \cdot \mathbf{H} \\ \mathbf{D} = \underline{\epsilon} \cdot \mathbf{E} + \underline{\xi} \cdot \mathbf{H} \end{cases} \tag{39}$$

its complementary medium is characterized by the following constitutive tensors:

$$\begin{cases} \underline{\mu}^c = \underline{\mu}^t \\ \underline{\epsilon}^c = \underline{\epsilon}^t \\ \underline{\zeta}^c = -\underline{\xi}^t \\ \underline{\xi}^c = -\underline{\zeta}^t \end{cases} \tag{40}$$

In (40) the superscript t stands for transposed tensor form. The medium is reciprocal if the complementary medium is identical to the original one. Bianisotropic media that satisfy the symmetry conditions are reciprocal if $\underline{\xi}$ and $\underline{\zeta}$ are purely imaginary matrices. It is easy to show that the pseudochiral medium is reciprocal. So, as in the case of the isotropic slab [18], the elements $\tilde{G}_{xy}, \tilde{G}_{zy}$ of the spectral Green's dyad can be obtained by applying the Parsevaal theorem to (38):

$$\tilde{G}_{ij}(\alpha, y_2, \beta|y_1) = \tilde{G}_{ji}(\alpha, y_1, \beta|y_2) \qquad (i = y; j = x, z) \tag{41}$$

If we, now, consider the transmission-line equations and the discontinuity relations appropriate to the point-source excitation case, there are no difficulties to generalize the $\mathrm{TM}(\hat{y})$ equivalent circuit to the case of a $\hat{y}$-oriented electric source and derive the $\tilde{G}_{yy}$ term.

3.2 Radiated Electric Field

In order to present an example of determination of the radiated field evaluated by applying the spectral theory, we consider an electric point-source located in the $x - z$ plane:

$$\mathbf{J} = \delta_0(x)\delta_0(y + h)\delta_0(z)(J_x\hat{\mathbf{x}} + J_z\hat{\mathbf{z}}) \tag{42}$$

The spatial electric field radiated in the spherical coordinate system can be evaluated by appropriately applying the equivalence theorem in the interface plane $y = 0$. Following such an approach the radiated electric field is given by:

$$\begin{cases} E_\theta(r, \theta, \phi) \equiv \dfrac{e^{-j\omega\sqrt{\epsilon\mu}\, r}}{r} \sin(\phi)\tilde{E}_z(\alpha', 0, \beta') \\ E_\phi(r, \theta, \phi) \equiv \dfrac{e^{-j\omega\sqrt{\epsilon\mu}\, r}}{r} \\ \qquad \cdot \left[\sin(\theta)\tilde{E}_x(\alpha', 0, \beta') + \cos(\theta)\cos(\phi)\tilde{E}_z(\alpha', 0, \beta')\right] \end{cases} \tag{43}$$

where

$$\begin{cases} \tilde{E}_x(\alpha', 0, \beta') = \tilde{G}_{xx,3}(\alpha', 0, \beta')J_x + \tilde{G}_{xz,3}(\alpha', 0, \beta')J_z \\ \tilde{E}_z(\alpha', 0, \beta') = \tilde{G}_{zx,3}(\alpha', 0, \beta')J_x + \tilde{G}_{zz,3}(\alpha', 0, \beta')J_z \end{cases} \tag{43a}$$

$$\begin{cases} \alpha' = \omega\sqrt{\epsilon\mu}\sin(\theta)\cos(\phi) \\ \beta' = \omega\sqrt{\epsilon\mu}\cos(\theta) \end{cases} \tag{43b}$$

The expression obtained for the radiated field is cumbersome to treat. However, when θ and ϕ are fixed to some particular values, which provide much insight into the physical properties of the medium,

the expression for the radiated field can be simplified. It is of interest to study the behavior of the electric field radiated on the horizon plane, that is the $x-z\,(\phi=0,\pi)$ plane. In this plane the electric far-field has the expression:

$$\begin{cases} E_\theta(r,\theta,\phi=0,\pi)=0 \\ E_\phi(r,\theta,\phi=0,\pi)\equiv \dfrac{e^{-j\omega\sqrt{\epsilon\mu}\ r}}{r}\Big\{\sin(\theta)\tilde{E}_x\left[\pm\omega\sqrt{\epsilon\mu}\sin(\theta)\right] \\ \qquad\qquad \pm\cos(\theta)\tilde{E}_z\left[\pm\omega\sqrt{\epsilon\mu}\sin(\theta)\right]\Big\} \end{cases} \tag{44}$$

The electric field radiated on the $x-z$ plane is, generally, zero. For particular values of the incidence angle, depending on the electromagnetic parameters of the two media, the radiated waves can propagate along the interface plane. In contrast of the isotropic case, due to the bianisotropy of the pseudochiral slab, the conditions for the radiation on the $x-z$ plane are not the same when we consider the radiation along the $\hat{x}$-axis or along the $\hat{z}$-axis. Different conditions hold, also, for the ordinary and for the extraordinary waves. Along the $\hat{z}$-axis of the $x-z$ plane, when $\theta=0,\pi$, the radiated pattern $\Lambda(\theta=0,\pi,\phi=0,\pi)=re^{-j\omega\sqrt{\epsilon\mu}\ r}\tilde{E}_z(r,\theta=0,\pi,\phi=0,\pi)$ for a pseudochiral grounded slab depends linearly on $k_2'(\theta=0,\pi,\phi=0,\pi)$. Since $k_2'(\theta=0,\pi,\phi=0,\pi)=k_2'(0,\pm\omega\sqrt{\epsilon\mu})=0$, as expected, the radiated pattern along the $\hat{z}$-axis of the horizon plane is, generally, zero unless $k_y'd=jn\pi\quad(n\in I)$, that is:

$$\begin{cases} d=d_1=\sqrt{\dfrac{\epsilon_{yy}}{\epsilon_{zz}}}\,\dfrac{n\pi}{\omega\sqrt{\mu_{xx}\epsilon_{yy}-\mu\epsilon}} \\ d=d_2=\sqrt{\dfrac{\mu_{yy}}{\mu_{zz}}}\,\dfrac{n\pi}{\omega\sqrt{\mu_{yy}\epsilon_{xx}-\mu\epsilon}} \end{cases} \quad \text{with} \quad \begin{cases} \mu_{xx}\epsilon_{yy}>\mu\epsilon & \text{for } d_1 \\ \mu_{yy}\epsilon_{xx}>\mu\epsilon & \text{for } d_2 \end{cases} \tag{45}$$

When the first of (45) holds, the ordinary wave propagates in the $x-z$ plane along the $\hat{z}$-axis. When the second of (45) holds, it is the extraordinary wave that propagates in the $x-z$ plane along the $\hat{z}$-axis. On the $\hat{z}$-axis of the horizon plane the modulus of the radiated pattern depends, in short only on J_z and ϵ_{zz} :

$$|\Lambda(\theta = 0, \pi, \phi = 0, \pi)| \equiv \left|\tilde{E}_z(0, 0, \pm\omega\sqrt{\epsilon\mu})\right|$$
$$\equiv \left|\frac{\delta'_{TM}(0, \pm\omega\sqrt{\epsilon\mu})}{j\omega\epsilon_{zz}} \sin\left(n\pi\frac{h}{d}\right) J_z\right| \qquad (n \in I) \tag{46}$$

Along the $\hat{x}$-axis of the $x - z$ plane, when $(\theta = \frac{\pi}{2}, \phi = 0, \pi)$ the radiated pattern $\Lambda(\theta = \frac{\pi}{2}, \phi = 0, \pi) = re^{j\omega\sqrt{\epsilon\mu}r}\tilde{E}_x(r, \theta = \frac{\pi}{2}, \phi = 0, \pi)$ for a pseudochiral grounded slab, once again, depends linearly on $k'_2(\theta = \frac{\pi}{2}, \phi = 0, \pi)$. Since $k'_2(\theta = \frac{\pi}{2}, \phi = 0, \pi) = k'_2(\pm\omega\sqrt{\epsilon\mu}, 0) = 0$, as expected, the radiated pattern along the $\hat{x}$-axis of the $x - z$ plane is, generally, zero. In this case the condition of radiation on the $x - z$ plane is:

$$\begin{aligned}&\left[\epsilon^2\mu^2\mu_{xx}\epsilon_{cc} - \epsilon\mu\mu_{xx}(\mu_{yy}\epsilon_{xx}\epsilon_{zz} + \mu_{zz}\epsilon_{cc}\epsilon_{yy})\right.\\ &\qquad \left. + \mu_{xx}\mu_{yy}\mu_{zz}\epsilon_{xx}\epsilon_{yy}\epsilon_{zz}\right](\omega d)^4 \\ &+(\mu_{xx}\epsilon_{yy}s_{xz} - \epsilon\mu s_{xy})(n\pi\omega d)^2 + \mu_{yy}\epsilon_{yy}(n\pi)^4 = 0 \qquad (n \in I)\end{aligned} \tag{47}$$

The solutions of (47) point out the existence of two positive values of d, the first one associated to the ordinary wave and the second one associated to the extraordinary wave. On the $\hat{x}$-axis of the horizon plane the modulus of the radiated pattern depends, in short only on J_x and ϵ_{xx}:

$$\left|\Lambda(\theta = \frac{\pi}{2}, \phi = 0, \pi)\right| \equiv \left|\tilde{E}_x(\pm\omega\sqrt{\epsilon\mu}, 0, 0)\right|$$
$$\equiv \left|\frac{\delta'_{TM}(\pm\omega\sqrt{\epsilon\mu}, 0)}{j\omega\epsilon_{xx}} \sin\left(n\pi\frac{h}{d}\right) J_x\right| \qquad (n \in I) \tag{48}$$

Conditions (45) and (47) generalize the corresponding ones for isotropic, bi-isotropic and anisotropic grounded slabs. It should be noted that, when:

$$\begin{cases} \Omega_{c1}^2 = \dfrac{[2\epsilon_{yy}\epsilon_{zz}\mu_{xx}\mu_{yy} - \epsilon\mu(\epsilon_{yy}\mu_{xx} + \epsilon_{zz}\mu_{yy})][\epsilon\mu(\epsilon_{xx} + \epsilon_{zz}) - \epsilon_{yy}s_{xz}]}{\epsilon_{yy}\mu_{xx}\mu_{yy}\epsilon\mu(\epsilon\mu - \epsilon_{yy}\mu_{zz})} \\ \Omega_{c2}^2 = \dfrac{[2\epsilon_{xx}\epsilon_{yy}\mu_{yy}\mu_{zz} - \epsilon\mu(\epsilon_{xx}\mu_{yy} + \epsilon_{yy}\mu_{zz})][\epsilon\mu(\mu_{xx} + \mu_{zz}) - \mu_{yy}s_{xz}]}{\mu_{xx}\mu_{yy}^2\epsilon\mu(\epsilon\mu - \epsilon_{yy}\mu_{zz})} \end{cases} \tag{49}$$

the radiation of the electric field on the $x-z$ plane occurs, for the same value of d (d_1, d_2 respectively), both along the $\widehat{x}$- and the $\widehat{z}$-direction. Then, by varying in an appropriate way the value of the pseudochirality admittance, it is possible to allow or to avoid the radiation of the electric field along two perpendicular directions of the $x-z$ plane.

Similarly, when the thickness of the pseudochiral slab is:

$$d_3 = \frac{n\pi}{\omega\sqrt{\mu\epsilon}}\sqrt{\frac{s_{xy}+s_{yz}}{\epsilon_{cc}\mu_{xx} - \epsilon_{zz}\mu_{zz}}} \cdot \sqrt{\frac{\epsilon\mu - 2\dfrac{\epsilon_{yy}\mu_{yy}s_{xz}}{s_{xy}+s_{yz}}}{\epsilon\mu - \dfrac{\epsilon_{xx}\epsilon_{zz}\mu_{xx}\mu_{yy} + \mu_{zz}(\epsilon_{cc}\epsilon_{yy}\mu_{xx} - \epsilon_{zz}s_{xy})}{\epsilon_{cc}\mu_{xx} - \epsilon_{zz}\mu_{zz}}}} \qquad (n \in I) \tag{100}$$

the radiation of the electric field on the $x-z$ plane occurs, for the same value of the pseudochirality admittance Ω_c, both along the $\widehat{x}$ and the $\widehat{z}$-direction.

3.3 Numerical Examples of the Radiated Electric Field

In this subsection some examples of radiated patterns are shown for different values of the electromagnetic parameters of the pseudochiral slab under planar excitation conditions. Fig. 3.3.1 shows the radiation pattern in the $y-z$ plane ($\phi = \pi/2$) for an electric point-source aligned along the $\widehat{z}$-axis.

Fig. 3.3.2 and Fig. 3.3.3 show the radiation pattern in the $x-y$ plane ($\theta = \pi/2$) for an electric point-source aligned along the $\widehat{x}$-axis. The role of the pseudochirality can be examined by comparison with the chiral and isotropic cases (Fig. 3.3.4) from the point of view of the

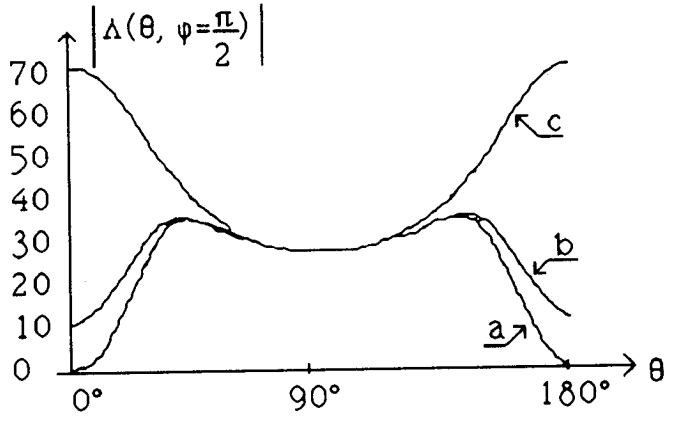

Figure 3.3.1 Examples of radiation on the horizon plane ($\epsilon_{xx} = 4\epsilon_0, \mu_{xx} = \mu_0, \mu_{yy} = 2\mu_0, \mu_{zz} = \mu_0, \Omega_c = 10^{-3}\Omega^{-1}, f = 10$ **GHz**, $d = 8 \cdot 10^{-3}$ **m**, $h = d/3, n = 1$; **a)** $\epsilon_{yy} = \epsilon_0, \epsilon_{zz} = \epsilon_0$; **b)** $\epsilon_{yy} = 1.1\epsilon_0, \epsilon_{zz} = 1.1\epsilon_0$; **c)** $\epsilon_{yy} = \epsilon_{zz} = 1.5\epsilon_0$).

radiation. From Fig. 3.3.4 it is observed that the pseudochiral material exhibits an increased directivity in the radiation pattern.

Finally, in Fig. 3.3.5 we show the effect of the chirality admittance ξ_c on the radiation along the $\hat{z}$-axis of the horizon plane. For some practical applications (for example: planar integrated antenna arrays) it is important to know and control the radiation on the horizon plane through the ξ_c parameter. According to (44), the value of the far-field radiated by a chiral grounded slab along the $\hat{z}$-axis of the horizon plane is given by [19]:

$$\left|\Lambda(\theta = 0, \pi, \phi = \frac{\pi}{2})\right| = \frac{\frac{\lambda\eta}{2d}\sqrt{(\epsilon_r - 1)}}{\sqrt[4]{1 + \left[\frac{\epsilon_r + 1}{\epsilon_r - 1}\right]^2 \frac{\eta^2\xi_c^2}{1 + \eta^2\xi_c^2}}} \qquad (n \neq 0 \in I) \tag{51}$$

where it is well evident the role of the chirality admittance ξ_c. A general reduction of the radiation in the $\hat{z}$-axis is observed, when a chiral slab is used.

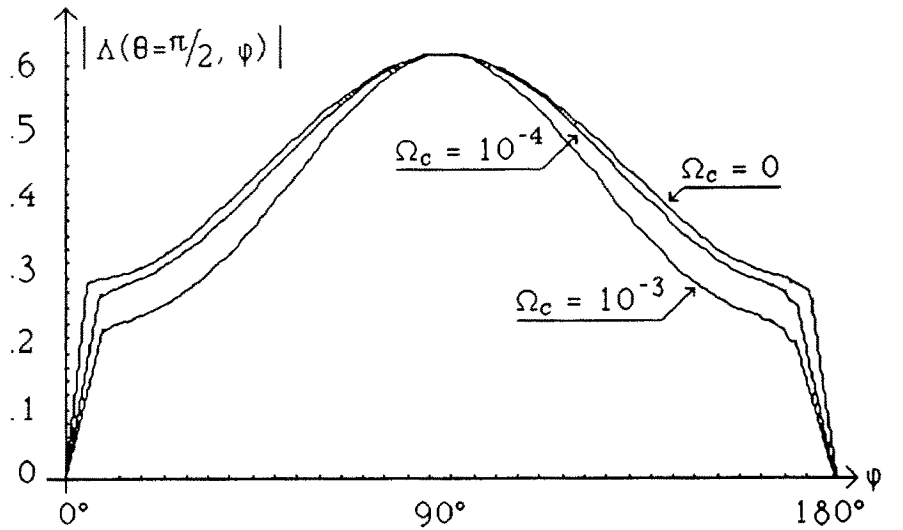

Figure 3.3.2 Radiated patterns in the $x-y$ plane for different values of the pseudochiral admittance Ω_c ($\epsilon_{xx} = 4\epsilon_0, \epsilon_{yy} = \epsilon_{zz} = 1.5\epsilon_0, \mu_{xx} = \mu_{zz} = \mu_0, \mu_{yy} = 2\mu_0, f = 10$ GHz, $d = 1.57 \cdot 10^{-3}$ m, $h = d/3$).

4. Discussion

In this paper we have generalized the spectral domain Immittance Matrix Approach to the case of bianisotropic layers. Starting from the Maxwell's equations, written in the two-dimensional Fourier domain, we have recognized that, when the constitutive tensors satisfy some general topological conditions (12), by introducing appropriate proportionality relations (17) between the transverse components, the spectral electromagnetic field in an unbounded bianisotropic medium admits a simple solution in terms of $\mathbf{TE}(\widehat{y})$ and $\mathbf{TM}(\widehat{y})$ waves, which satisfy transmission-line equations. In this way we have obtained an important result: when the constitutive tensors assume form (12), the Maxwell's equations in the two-dimensional Fourier domain provides the circuit modelization of the medium.

These results have been applied 1) to an unbounded pseudochiral medium; 2) to a pseudochiral grounded slab embedded in an un-

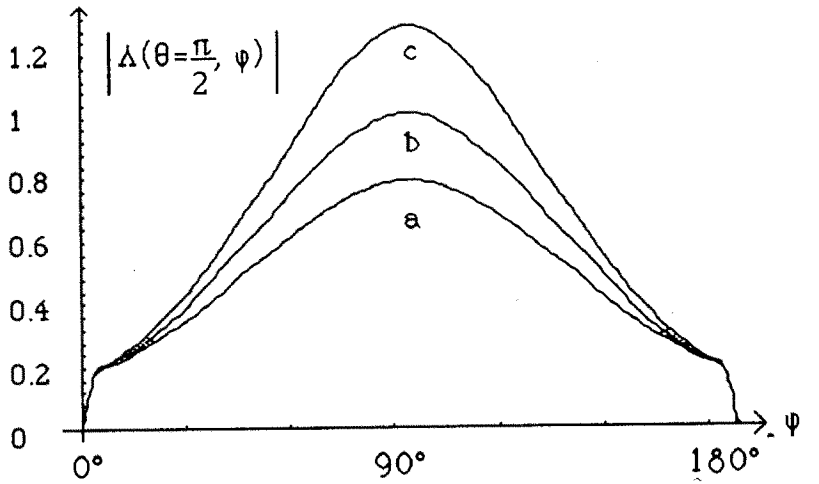

Figure 3.3.3 Radiated patterns in the $x-y$ plane for different values of ϵ_{xx}. ($\epsilon_{yy} = \epsilon_{zz} = \epsilon_0, \mu_{xx} = \mu_{zz} = 1.5\mu_0, \mu_{yy} = 2\mu_0, \Omega_c = 10^{-3}\Omega^{-1}, f = 10$ GHz, $d = 1.57 \cdot 10^{-3}$ m, $h = d/3$; a) $\epsilon_{xx} = 6\epsilon_0$; b) $\epsilon_{xx} = 8\epsilon_0$; c) $\epsilon_{xx} = 10\epsilon_0$).

bounded isotropic half-space, fed by an electric planar deep point-source.

In respect of the item 1) the proportionality relations (17) lead to the decoupling of the spectral electromagnetic field in $\mathbf{TE}(\widehat{y})$ and $\mathbf{TM}(\widehat{y})$ waves satisfying the transmission-line equations. The determination of the spectral wavenumbers k_y has allowed us to recognize the existence of a double mode of propagation associable to an ordinary/extraordinary wave, strongly affected by the value of the pseudochirality admittance. In studying the bimodal propagation we have recognized that the spectral field can be subdivided in surface (k_y real) and volume (k_y complex) waves. We found in implicit form the zeros of k_y and the conditions which must be satisfied by the electromagnetic parameters in order to reduce the two waves of propagation in a single one.

In 2) the introduction of the equivalent circuits has been used to evaluate the spectral electric Green's dyad associated with the pseudochiral grounded slab in a simple and closed analytical form which can be easily managed by the designer. In the expressions of the ele-

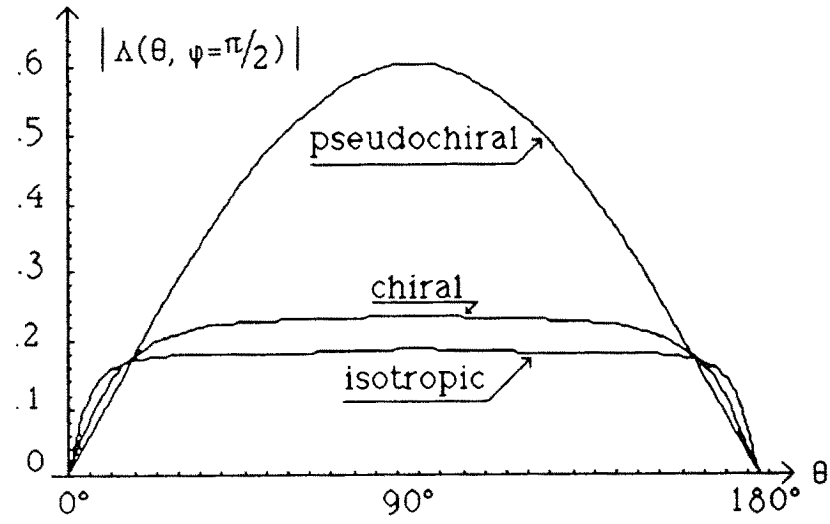

Figure 3.3.4 Radiated patterns in the $y-z$ plane for different media. ($\epsilon_{xx} = \epsilon_{yy} = \epsilon_{zz} = \epsilon_0, \mu_{xx} = \mu_{zz} = \mu_{yy} = \mu_0, f = 10$ **GHz**, $d = 1.57 \cdot 10^{-3}$ **m**, $h = d/3, \xi_c = 10^{-3}\Omega^{-1}, \Omega_c = 10^{-3}\Omega^{-1}$).

ments of the spectral electric Green's dyad the effect of the separation of the spectral electromagnetic field in $\mathbf{TE}(\widehat{y})$ and $\mathbf{TM}(\widehat{y})$ waves is well evident. It is important to note that the expression of the spectral electric Green's dyad is not formally affected by the complexity of the layer; so the spectral Green's dyad is formally the same both for an isotropic and a pseudochiral grounded slab. The differences are all constrained in the formulation of the secondary constants of the $\mathbf{TE}(\widehat{y})$ and $\mathbf{TM}(\widehat{y})$ equivalent transmission line, proper of the grounded slab.

Another feature of the Immittance Matrix Approach is that to derive directly, in a closed form, without evaluating Sommerfeld-type integrals, the electric field radiated by the grounded slab.

The presented theory allowed, also, to derive the conditions that must be respected by the electromagnetic constants of the medium, thickness of the slab, position of the source and working frequency in order to control the radiation on the horizon plane. The conditions for the radiation on the horizon plane along the $\widehat{x}$- and along the $\widehat{z}$-axis, for the ordinary and for the extraordinary waves are shown in subsection 3.2. It is to be pointed out that in literature there is no

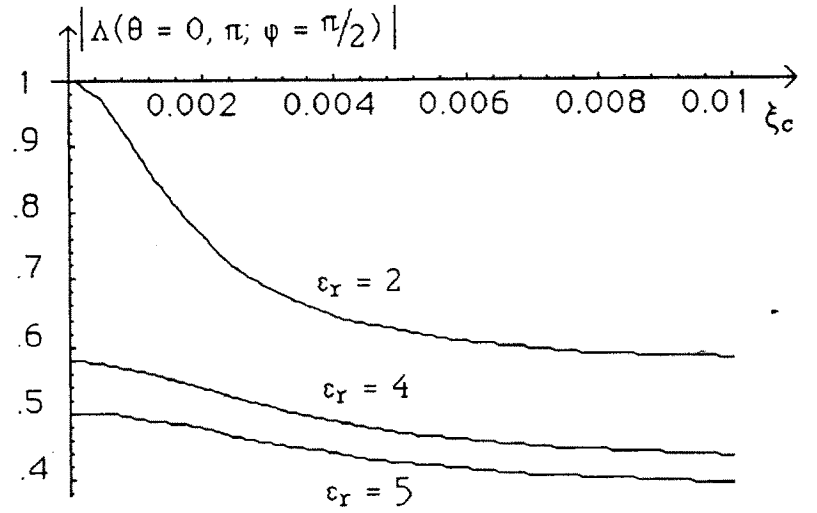

Figure 3.3.5 Values of the radiated pattern normalized to λ/d versus ξ_c for different ϵ_r in the $\widehat{z}$-axis (λ = wavelength, d = thickness of the slab).

mention of the conditions of radiation on the horizon plane of such bianisotropic structures. In subsection 3.3 several numerical computations of the electric radiated field are shown, in the case of electric $\widehat{x}$- and $\widehat{z}$-oriented point-source.

In Fig. 3.3.1 is reported the case of radiation maxima at the horizon for an electric $\widehat{z}$-oriented point-source, under the validity of (45) and (46) with $n\frac{h}{d} \neq q\,[(n,q) \in \mathbf{I}]$. As shown in Fig. 3.3.2, the electric fields radiated by an electric $\widehat{x}$-oriented point-source present a symmetry with respect to the $\widehat{y}$-axis ($\phi = \pi/2$). The radiation maxima progressively widen towards the $\widehat{x}$-axis ($\phi = 0, \pi$) for decreasing values of Ω_c. In Fig. 3.3.3 several radiated patterns in the $x - y$ plane for different values of ϵ_{zz} are plotted. As it is well evident, the amplitudes of the radiated patterns are strongly affected by ϵ_{xx}.

In general, the radiated patterns depend, when the electric point-source is aligned along the $\widehat{z}$-axis only on the $\epsilon_{yy}, \epsilon_{zz}, \mu_{xx}$ parameters, while, when the electric point-source is aligned along the $\widehat{x}$-axis, on the $\epsilon_{xx}, \mu_{yy}, \mu_{zz}$ parameters.

To study the role of the pseudochirality (Ω_c) admittance and the chirality (ξ_c) admittance in these planar structures Figs. 3.3.4 and 3.3.5 have been presented. Fig. 3.3.4 gives a comparison among the radiated patterns for the three different cases of isotropic, chiral and Ω slabs fed by electric horizontal point-sources. The comparison shows an increase of the value and directivity of the far-field in the $y-z$ plane for the Ω slabs. This effect can be explained with the fact that, on the contrary of a chiral material, where the induced dipoles are randomly distributed in the host dielectric medium, in an Ω-medium all the induced dipoles lie in the $x-y$ plane. Therefore, the pseudochirality Ω_c admittance controls in a stronger way than the chirality ξ_c admittance the value and the directivity of the radiated pattern in the $y-z$ plane. Fig.3.3.5 gives some information about the reduction of the radiation in the horizon plane achieved with chiral slabs. This figure shows that, under certain circumstances, this radiation can be lowered by using chiral slabs in conjunction with high values of the permittivity ϵ_r. This means that in the far-field region the effect of the surface electromagnetic waves, traveling with wavenumbers parallel to the interface plane, together with the volume ones becomes negligible with increased chirality. More details about it can be obtained from the expressions of the spectral dyadic Green's function given in [19]. This result may lead to an increased radiation efficiency of the structure, when a metallic patch is photoetched on the interface plane, that is when chiral slabs are used in applications, such as printed antenna arrays.

5. Conclusion

In this paper we have studied the circuit modeling of a planar structure with a general bianisotropic slab by using the transmission-line analogy. This important result has been found: when the constitutive tensors assume form (12), the circuit modelization is always possible. We have applied this result to the study case of a bianisotropic pseudochiral Ω grounded slab embedded in an unbounded isotropic half-space, fed by an electric planar deep point-source. The study case has been extensively investigated by deriving in a closed analytical form the spectral (Fourier) dyadic Green's function of the structure and by obtaining important information on the properties of radiation

of the structure together with conditions to control the radiation on the horizon plane.

Numerical evaluations of planar structure radiated fields, backed with a slab of different anisotropic material, have been presented along with important information on the electromagnetic constants of the medium, the thickness of the slab, the position of the source and working frequency. Lastly, a comparison among the radiated patterns of isotropic, chiral and Ω slabs has been provided, together with some information about the reduction of the radiation in the horizon plane of chiral slabs. A reduction of the radiation on the horizon plane can be obtained by using chiral slabs with high permittivity.

Appendix

Expressions of the c_{ij} terms $(i,j = 1,2,3,4)$ for a very general bianisotropic medium

$$c_{11} = -j\xi^2 \frac{\mu_{yy}}{\omega(\epsilon_{yy}\mu_{yy} - \sigma_{yy}\tau_{yy})} + j\xi \frac{\mu_{yu}\sigma_{yy} + \mu_{uy}\tau_{yy} - \mu_{yy}(\tau_{uy} + \sigma_{yu})}{\epsilon_{yy}\mu_{yy} - \sigma_{yy}\tau_{yy}}$$
$$- j\omega \left[\frac{\epsilon_{yy}(\mu_{uy}\mu_{yu} - \mu_{uu}\mu_{yy}) + \tau_{yy}(\sigma_{yy}\mu_{uu} - \sigma_{yu}\mu_{uy})}{\epsilon_{yy}\mu_{yy} - \sigma_{yy}\tau_{yy}} \right.$$
$$\left. + \frac{\tau_{uy}(\sigma_{yu}\mu_{yy} - \sigma_{yy}\mu_{yu})}{\epsilon_{yy}\mu_{yy} - \sigma_{yy}\tau_{yy}} \right]$$

$$c_{12} = j\xi \frac{\mu_{yv}\sigma_{yy} - \mu_{yy}\sigma_{yv}}{\epsilon_{yy}\mu_{yy} - \sigma_{yy}\tau_{yy}}$$
$$- j\omega \left[\frac{\epsilon_{yy}(\mu_{uy}\mu_{yv} - \mu_{uv}\mu_{yy}) + \tau_{uy}(\mu_{yy}\sigma_{yv} - \mu_{yv}\sigma_{yy})}{\epsilon_{yy}\mu_{yy} - \sigma_{yy}\tau_{yy}} \right.$$
$$\left. + \frac{\tau_{yy}(\mu_{uv}\sigma_{yy} - \mu_{uy}\sigma_{yv})}{\epsilon_{yy}\mu_{yy} - \sigma_{yy}\tau_{yy}} \right]$$

$$c_{13} = -j\xi\frac{(\epsilon_{yv}\mu_{yy} - \sigma_{yy}\tau_{yv})}{\epsilon_{yy}\mu_{yy} - \sigma_{yy}\tau_{yy}} + j\omega\left[\frac{\epsilon_{yy}(\mu_{yy}\tau_{uv} - \mu_{uy}\tau_{yv}) + \epsilon_{yv}(\mu_{uy}\tau_{yy} - \mu_{yy}\tau_{uy})}{\epsilon_{yy}\mu_{yy} - \sigma_{yy}\tau_{yy}} + \frac{\sigma_{yy}(\tau_{uy}\tau_{yv} - \tau_{uv}\tau_{yy})}{\epsilon_{yy}\mu_{yy} - \sigma_{yy}\tau_{yy}}\right]$$

$$c_{14} = -j\xi^2\frac{\sigma_{yy}}{\omega(\epsilon_{yy}\mu_{yy} - \sigma_{yy}\tau_{yy})} + j\xi\frac{\epsilon_{yy}\mu_{uy} - \epsilon_{yu}\mu_{yy} + \sigma_{yy}(\tau_{yu} - \tau_{uy})}{\epsilon_{yy}\mu_{yy} - \sigma_{yy}\tau_{yy}} + j\omega\left[\frac{\mu_{yy}(\epsilon_{yy}\tau_{uu} - \epsilon_{yu}\tau_{uy}) + \tau_{yu}(\sigma_{yy}\tau_{uy} - \epsilon_{yy}\mu_{uy})}{\epsilon_{yy}\mu_{yy} - \sigma_{yy}\tau_{yy}} + \frac{\tau_{yy}(\epsilon_{yu}\mu_{uy} - \sigma_{yy}\tau_{yu})}{\epsilon_{yy}\mu_{yy} - \sigma_{yy}\tau_{yy}}\right]$$

$$c_{21} = j\xi\frac{\mu_{yy}\tau_{vy} - \mu_{vy}\tau_{yy}}{\epsilon_{yy}\mu_{yy} - \sigma_{yy}\tau_{yy}} + j\omega\left[\frac{\epsilon_{yy}(\mu_{vy}\mu_{yu} - \mu_{vu}\mu_{yy}) + \tau_{vy}(\mu_{yy}\sigma_{yu} - \mu_{yu}\sigma_{yy})}{\epsilon_{yy}\mu_{yy} - \sigma_{yy}\tau_{yy}} + \frac{\tau_{yy}(\mu_{vu}\sigma_{yy} - \mu_{vy}\sigma_{yu})}{\epsilon_{yy}\mu_{yy} - \sigma_{yy}\tau_{yy}}\right]$$

$$c_{22} = j\omega\left[\frac{\epsilon_{yy}(\mu_{vy}\mu_{yv} - \mu_{vv}\mu_{yy}) + \tau_{vy}(\mu_{yy}\sigma_{yv} - \mu_{yv}\sigma_{yy})}{\epsilon_{yy}\mu_{yy} - \sigma_{yy}\tau_{yy}} + \frac{\tau_{yy}(\mu_{vv}\sigma_{yy} - \mu_{vy}\sigma_{yv})}{\epsilon_{yy}\mu_{yy} - \sigma_{yy}\tau_{yy}}\right]$$

$$c_{23} = -j\omega \left[\frac{\epsilon_{yy}(\mu_{yy}\tau_{vv} - \mu_{vy}\tau_{yv}) + \tau_{vy}(\sigma_{yy}\tau_{yv} - \epsilon_{yv}\mu_{yy})}{\epsilon_{yy}\mu_{yy} - \sigma_{yy}\tau_{yy}} + \frac{\tau_{yy}(\epsilon_{yv}\mu_{vy} - \sigma_{yy}\tau_{vv})}{\epsilon_{yy}\mu_{yy} - \sigma_{yy}\tau_{yy}} \right]$$

$$c_{24} = -j\xi \frac{\epsilon_{yy}\mu_{vy} - \sigma_{yy}\tau_{vy}}{\epsilon_{yy}\mu_{yy} - \sigma_{yy}\tau_{yy}} - j\omega \left[\frac{\epsilon_{yy}(\mu_{yy}\tau_{vu} - \mu_{vy}\tau_{yu}) + \tau_{vy}(\sigma_{yy}\tau_{yu} - \epsilon_{yu}\mu_{yy})}{\epsilon_{yy}\mu_{yy} - \sigma_{yy}\tau_{yy}} + \frac{\tau_{yy}(\epsilon_{yu}\mu_{vy} - \sigma_{yy}\tau_{vu})}{\epsilon_{yy}\mu_{yy} - \sigma_{yy}\tau_{yy}} \right]$$

$$c_{31} = -j\xi \frac{(\epsilon_{vy}\mu_{yy} - \sigma_{vy}\tau_{yy})}{\epsilon_{yy}\mu_{yy} - \sigma_{yy}\tau_{yy}} + j\omega \left[\frac{\epsilon_{yy}(\mu_{yy}\sigma_{vu} - \mu_{yu}\sigma_{vy}) + \epsilon_{vy}(\mu_{yu}\sigma_{yy} - \mu_{yy}\sigma_{yu})}{\epsilon_{yy}\mu_{yy} - \sigma_{yy}\tau_{yy}} + \frac{\tau_{yy}(\sigma_{vy}\sigma_{yu} - \sigma_{vu}\sigma_{yy})}{\epsilon_{yy}\mu_{yy} - \sigma_{yy}\tau_{yy}} \right]$$

$$c_{32} = j\omega \left[\frac{\epsilon_{yy}(\mu_{yy}\sigma_{vv} - \mu_{yv}\sigma_{vy}) + \epsilon_{vy}(\mu_{yv}\sigma_{yy} - \mu_{yy}\sigma_{yv})}{\epsilon_{yy}\mu_{yy} - \sigma_{yy}\tau_{yy}} + \frac{\tau_{yy}(\sigma_{vy}\sigma_{yv} - \sigma_{vv}\sigma_{yy})}{\epsilon_{yy}\mu_{yy} - \sigma_{yy}\tau_{yy}} \right]$$

$$c_{33} = -j\omega \left[\frac{\mu_{yy}(\epsilon_{vy}\epsilon_{yv} - \epsilon_{vv}\epsilon_{yy}) + \tau_{yv}(\epsilon_{yy}\sigma_{vy} - \epsilon_{vy}\sigma_{yy})}{\epsilon_{yy}\mu_{yy} - \sigma_{yy}\tau_{yy}} + \frac{\tau_{yy}(\epsilon_{vv}\sigma_{yy} - \epsilon_{yv}\sigma_{vy})}{\epsilon_{yy}\mu_{yy} - \sigma_{yy}\tau_{yy}} \right]$$

$$c_{34} = j\xi \frac{(\epsilon_{yy}\sigma_{vy} - \epsilon_{vy}\sigma_{yy})}{\epsilon_{yy}\mu_{yy} - \sigma_{yy}\tau_{yy}} - j\omega \left[\frac{\mu_{yy}(\epsilon_{vy}\epsilon_{yu} - \epsilon_{vu}\epsilon_{yy}) + \tau_{yu}(\epsilon_{yy}\sigma_{vy} - \epsilon_{vy}\sigma_{yy})}{\epsilon_{yy}\mu_{yy} - \sigma_{yy}\tau_{yy}} + \frac{\tau_{yy}(\epsilon_{vu}\sigma_{yy} - \epsilon_{yu}\sigma_{vy})}{\epsilon_{yy}\mu_{yy} - \sigma_{yy}\tau_{yy}} \right]$$

$$c_{41} = j\xi^2 \frac{\tau_{yy}}{\omega(\epsilon_{yy}\mu_{yy} - \sigma_{yy}\tau_{yy})} + j\xi \frac{\epsilon_{uy}\mu_{yy} - \epsilon_{yy}\mu_{yu} + \tau_{yy}(\sigma_{yu} - \sigma_{uy})}{\epsilon_{yy}\mu_{yy} - \sigma_{yy}\tau_{yy}} - j\omega \left[\frac{\epsilon_{yy}(\mu_{yy}\sigma_{uu} - \mu_{yu}\sigma_{uy}) + \epsilon_{uy}(\mu_{yu}\sigma_{yy} - \mu_{yy}\sigma_{yu})}{\epsilon_{yy}\mu_{yy} - \sigma_{yy}\tau_{yy}} + \frac{\tau_{yy}(\sigma_{uy}\sigma_{yu} - \sigma_{uu}\sigma_{yy})}{\epsilon_{yy}\mu_{yy} - \sigma_{yy}\tau_{yy}} \right]$$

$$c_{42} = -j\xi \frac{\epsilon_{yy}\mu_{yv} - \sigma_{yv}\tau_{yy}}{\epsilon_{yy}\mu_{yy} - \sigma_{yy}\tau_{yy}} - j\omega \left[\frac{\epsilon_{yy}(\mu_{yy}\sigma_{uv} - \mu_{yv}\sigma_{uy}) + \epsilon_{uy}(\mu_{yu}\sigma_{yy} - \mu_{yy}\sigma_{yv})}{\epsilon_{yy}\mu_{yy} - \sigma_{yy}\tau_{yy}} + \frac{\tau_{yy}(\sigma_{uy}\sigma_{yv} - \sigma_{uv}\sigma_{yy})}{\epsilon_{yy}\mu_{yy} - \sigma_{yy}\tau_{yy}} \right]$$

$$c_{43} = j\xi \frac{(\epsilon_{yv}\tau_{yy} - \epsilon_{yy}\tau_{yv})}{\epsilon_{yy}\mu_{yy} - \sigma_{yy}\tau_{yy}} + j\omega \left[\frac{\mu_{yy}(\epsilon_{uy}\epsilon_{yv} - \epsilon_{uv}\epsilon_{yy}) + \tau_{yv}(\epsilon_{yy}\sigma_{uy} - \epsilon_{uy}\sigma_{yy})}{\epsilon_{yy}\mu_{yy} - \sigma_{yy}\tau_{yy}} + \frac{\tau_{yy}(\epsilon_{uv}\sigma_{yy} - \epsilon_{yv}\sigma_{uy})}{\epsilon_{yy}\mu_{yy} - \sigma_{yy}\tau_{yy}} \right]$$

$$c_{44} = j\xi^2 \frac{\epsilon_{yy}}{\omega(\epsilon_{yy}\mu_{yy} - \sigma_{yy}\tau_{yy})} + j\xi \frac{\epsilon_{uy}\sigma_{yy} + \epsilon_{yu}\tau_{yy} - \epsilon_{yy}(\tau_{yu} + \sigma_{uy})}{\epsilon_{yy}\mu_{yy} - \sigma_{yy}\tau_{yy}}$$
$$+ j\omega \left[\frac{\mu_{yy}(\epsilon_{uy}\epsilon_{yu} - \epsilon_{uu}\epsilon_{yy}) + \tau_{yu}(\epsilon_{yy}\sigma_{uy} - \epsilon_{uy}\sigma_{yy})}{\epsilon_{yy}\mu_{yy} - \sigma_{yy}\tau_{yy}} \right.$$
$$\left. + \frac{\tau_{yy}(\epsilon_{uu}\sigma_{yy} - \epsilon_{yu}\sigma_{uy})}{\epsilon_{yy}\mu_{yy} - \sigma_{yy}\tau_{yy}} \right]$$

References

1. Mu, T. C., H. Ogawa, and T. Itoh, "Characteristics of multiconductor, asymmetric, slow-wave microstrip transmission lines," *IEEE Trans. Microwave Theory Tech.*, Vol. MTT-34, 1471–1477, 1986.
2. Das, N. K., and D. M. Pozar, "A generalized spectral-domain Green's function for multilayer dielectric substrates with applications to multilayer transmission lines," *IEEE Trans. Microwave Theory Tech.*, Vol. MTT-35, 326–335, 1987.
3. Alexopulos, N. G., "Integrated-circuit structures on anisotropic substrates," *IEEE Trans. Microwave Theory Tech.*, Vol. MTT-33, 847–881, 1985.
4. Hansen, R. C., "Antenna application of superconductors," *IEEE Trans. Microwave Theory Tech.*, Vol. MTT-39, 1508–1512, 1991.
5. Mosig, J. R., "Arbitrarily shaped microstrip structures and their analysis with a mixed potential integral equation," *IEEE Trans. Ant. Pro.*, Vol. AP-36, 314–323, 1988.
6. Koul, S. K., and B. Bhat, "Inverted microstrip and suspended microstrip with anisotropic substrates," *Proc. IEEE,* Vol. 70, 1230–1231, 1982.
7. Krowne, C. M., "Fourier transformed matrix method of finding propagation characteristics of complex anisotropic layered media," *IEEE Trans. Microwave Theory Tech.*, Vol. MTT-32, 1617–1625, 1984.
8. Tsalamengas, S. C., and N. K. Uzunoglu, "Radiation from a dipole in the proximity of a general anisotropic grounded layer," *IEEE Trans. Ant. Pro.*, Vol. AP-33, 165–172, 1985.
9. Mesa, L. M., R. Marqués, and M. Horno, "A general algorithm for computing the bidimensional spectral Green's dyad in multilayered

complex bianisotropic media: the equivalent boundary method," *IEEE Trans. Microwave Theory Tech.,* Vol. MTT-39, 1640–1649, 1991.

10. Cano, G., F. Medina, and M. Horno, "Efficient spectral domain analysis of generalized multistrip lines in stratified media including thin, anisotropic, and lossy substrates," *IEEE Trans. Microwave Theory Tech.,* Vol. MTT-40, 217–227, 1992.
11. Engheta, N., and M. M. I. Saadoun, "Novel pseudo chiral or Ω medium and its applications," *Proceedings of PIERS 1991,* Cambridge, Massachusetts, USA, 339, 1991.
12. Saadoun, M. M. I., and N. Engheta, "Novel designs for reciprocal phase shifters using pseudochiral Ω-medium," *Proceedings of URSI Symposium 1991,* London, Ontario, 337, 1991.
13. Saadoun, M. M.I., and N. Engheta, "A reciprocal phase shifter using pseudochiral or Ω-medium," *Microwave Optical Technology Lett.,* Vol. 5, No. 4, 184–188,1992.
14. Saadoun, M. M. I., and N. Engheta, "The pseudochiral Ω- medium: what is it? and what can be used for?," *Proceedings of IEEE AP-S Intl Symposium,* Chicago, Vol. 4, 2038–2041,1992.
15. Mariotte, F., A. Fourrier-Lamer, and S. Zouhdi, "Absorbing polarisator shield having planar chiral patterns," Patent Number 526269, Date of Patent 28.06.1991.
16. Kong, J. A., "Theorems of bianisotropic media," *Proc. IEEE,* Vol. 60, 1036–1046, 1972.
17. Post, E. J., *Formal Structure of Electromagnetics,* North-Holland, Amsterdam, 1962.
18. Vegni, L., R. Cicchetti, and Capece, "Spectral dyadic Green's function formulation for planar integrated structures," *IEEE Trans. Ant. Pro.,* Vol. AP-36, 1057–1065, 1988.
19. Toscano, A., and L. Vegni, "Spectral dyadic Green's function formulation for planar integrated structures with a grounded chiral slab," *J. Electr. Waves Applic.,* Vol. 6, 751–769, 1992.
20. Toscano, A., and L. Vegni, "Spectral electromagnetic modeling of a planar integrated structure with general grounded anisotropic slab," *IEEE Trans. Ant. Pro.,* Vol. AP-41, 362–370, 1993.